

# Dynamics and longevity of an initially stratified mantle

Helge M. Gonnermann, Michael Manga, and A. Mark Jellinek

University of California, Berkeley, California, USA

Received 3 February 2002; revised 30 March 2002; accepted 8 April 2002; published 22 May 2002.

[1] We performed laboratory experiments of thermochemical convection in order to determine the rate at which an initially density-stratified, and hence layered, mantle will be homogenized. In the experiments, two layers of fluid with similar viscosities are superposed and heated from below. Initially, in the “stratified” regime, mechanical entrainment into both layers occurs by viscous coupling and theoretical models for the entrainment rate agree well with our experimental data. Over time entrainment and mixing reduce the density difference between the layers until the “doming” regime is reached. The density interface becomes unstable, thermal plumes of the dense fluid penetrate into the overlying layer and the entrainment rate reaches a constant. Applying our results to the Earth’s mantle, we confirm that it is possible for a compositionally distinct layer to persist over the age of the Earth, even if the initial density difference is less than 2%. *INDEX TERMS*: 8147 Evolution of the Earth: Planetary interiors (5430, 5724); 8124 Tectonophysics: Earth’s interior—composition and state (8105); 8120 Tectonophysics: Dynamics of lithosphere and mantle—general; 8121 Tectonophysics: Dynamics, convection currents and mantle plumes; 8130 Evolution of the Earth: Heat generation and transport

## 1. Introduction

[2] Some form of layering in the mantle due to compositional heterogeneity is often invoked to explain a variety of observations, including trace element and isotope systematics of mantle-derived basalts [e.g., *Turcotte et al.*, 2001], the Earth’s heat budget [e.g., *Kellogg et al.*, 1999], and seismological observations [e.g., *Saltzer et al.*, 2001]. While early models of layered convection associated layering with the upper and lower mantles, more recent seismological observations suggest that slabs sink deep into the mantle [e.g., *Grand et al.*, 1997]. Thus if the mantle is compositionally stratified, the dense layer must lie within the lower mantle and may be highly deformed [Becker et al., 1999; Kellogg et al., 1999]. A lower mantle with large-scale compositional heterogeneity is also not incompatible with a number of geophysical constraints [e.g., *Forte and Mitrovia*, 2001].

[3] In the absence of density stratification, mixing in the lower mantle is too efficient for significant portions to remain isolated over the lifetime of the Earth [e.g., *van Keken and Zhong*, 1999; *Hunt and Kellogg*, 2001]. Density stratification and resultant thermochemical convection, however, will alter the dynamics of the convective flow [Tackley, 1998] and mixing will be governed by the rate of entrainment across the density interface.

[4] Using analog experiments, *Davaille* [1999a] observed two styles of thermochemical convection: (1) a “stratified” regime; and (2) a “doming” regime, in which the density interface becomes highly deformed by rising and sinking dome-like flow structures. The latter can be stable for several “cycles” if the viscosity ratio,  $\gamma = \eta_l/\eta_u$ , exceeds one order of magnitude. Here  $\eta_l$  is the viscosity of dense (lower) fluid and  $\eta_u$  is the viscosity of light (upper) fluid. Figure 1 shows the range of  $\gamma$  and buoyancy parameter,  $B$ , over

which these two modes of convection occur. We define  $B = \Delta\rho/\rho\alpha\Delta T$ , where  $\Delta\rho$  is the difference in density between upper and lower fluids,  $\rho$  is the density of the lower fluid and  $\alpha$  is thermal expansivity. Here we use  $\Delta T = \Delta T_b$ , the temperature difference between the bottom of the tank and the lower fluid (Figure 2), because it characterizes the thermal buoyancy of hot rising plumes.

[5] The purpose of this paper is to extend previous studies of thermochemical convection by quantifying the rate of entrainment across the density interface over the complete evolution of a layer. We focus on  $\gamma$  close to unity because of the “lack of compelling evidence for a huge viscosity increase through the lower mantle” [Schubert et al., 2001, p. 240]. Moreover, the parameter range we consider (shown in Figure 1) has not been investigated in detail [Davaille, 1999a, 1999b]. We discuss observed convective regimes, the transition between regimes, as well as mechanics of entrainment. We show that existing scaling laws [Sleep, 1988; Davaille, 1999a, 1999b] are consistent with our data. Finally, we use our results to predict the lifetime of a hypothetical dense layer in the Earth’s mantle.

## 2. Experimental Method

[6] In numerical calculations it is challenging to resolve the small length scales at which entrainment takes place. In addition, it is often difficult, especially in 3-D simulations, to achieve Earth-like Rayleigh numbers ( $Ra = g\alpha\Delta T_b H^3/\kappa\eta_u$ , where  $g$  is acceleration due to gravity,  $H$  is total fluid depth and  $\kappa$  is thermal diffusivity). Therefore, we performed a series of analog experiments similar to those of *Olson and Kincaid* [1991], but at larger  $Ra$  with vigorous convection in both layers. The experiments are scaled to conditions appropriate to the Earth’s mantle ( $Ra \sim 10^7$ ), and viscous forces dominate inertial forces, i.e. Reynolds number  $Re = uH/\eta < 1$ , where  $u$  is a characteristic velocity.

[7] We conduct experiments in a glass tank (0.125 m  $\times$  0.250 m  $\times$  0.150 m high). The tank bottom is a 6.35 mm thick aluminum plate that is heated from below by an electrical resistance heater with a constant heat flux  $q$ . It is not isothermal, but lateral variations in temperature are always less than 8% of the total temperature difference throughout the tank. As a consequence of secular heating the experiments are transient, but on a time scale that is long compared to the time scale for plume formation (Figure 2). Sidewalls are insulated throughout the experiments, except when shadow-graph images of the convective flow are generated by projecting light through one side of the tank. The top of the convecting layer is at room temperature. Throughout the experiment temperatures are measured by thermocouples installed at the bottom of the tank and at different lateral and vertical positions within the convecting fluid. The thermocouples are removed for several control experiments to ensure that the observed flow is not influenced by the thermocouples. Corn syrup solutions or polybutene oils are used as working fluids. Because all our experiments provide similar results, we focus here on details of an experiment using dyed corn syrup as the dense (lower) fluid and corn syrup diluted with water as the light (upper) fluid.

[8] At the start of the experiment a layer of light fluid (0.125 m high) convects at  $Ra \sim 10^7$ . We then pour in a dense fluid which forms a layer (0.025 m high) at the bottom of the tank. Heating and vigorous convection cause the lower layer to increase in temper-

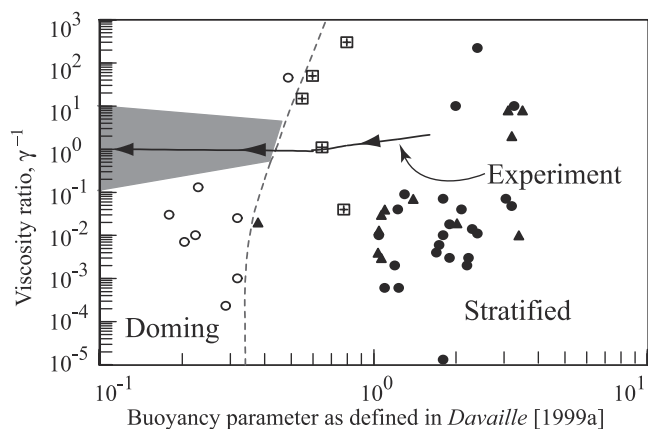


**Figure 1.** Convective regimes as a function of buoyancy parameter and viscosity ratio  $\gamma$  (after Figure 2 of *Davaille* [1999a]). The horizontal axis shows buoyancy parameter as defined by *Davaille* [1999a] using the temperature difference across the entire tank (we define the buoyancy parameter,  $B$ , based the temperature difference between the bottom of the tank and the lower fluid). Symbols represent individual experiments performed by *Davaille*. Black solid line with arrows labeled “Experiment” shows the range of parameter space traversed by the experiment shown in Figures 3a, 3c, and 4. The dashed line separates the stratified regime from the doming regime. The shaded area is the domain where viscosity ratios are insufficient to sustain a doming mode in *Davaille*’s experiments.

ature until a maximum temperature is reached. At this point  $B$  has a value of approximately 1.6, which is sufficient to obtain an initially stratified convective regime [*Olson and Kincaid*, 1991] and is similar to values suggested in previous studies [*Kellogg et al.*, 1999; *Forte and Mitrovica*, 2001]. Initially  $\gamma \approx 2.5$  and approaches 1 during the course of the experiment.

### 3. Results

#### 3.1. Flow Regimes and Entrainment

[9] Two regimes of thermochemical convection are observed, with a transition at  $B \approx 0.8$ . Values of  $B$  from our experiments are approximately a factor of 2 to 4 larger than those of *Davaille* [1999a, 1999b], who defined  $B$  using the temperature difference across the entire tank. Both sets of experiments are compatible once the difference in buoyancy parameter is taken into account.

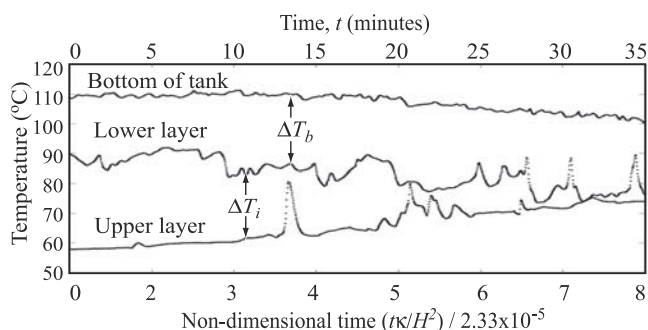


**Figure 2.** Temperature of upper layer, lower layer and bottom of the tank throughout the experiment.  $\Delta T_b$  was used to calculate  $Ra$  and  $B$ , while  $\Delta T_i$  was used to estimate  $\Delta\rho$ . At time  $t = 0$  temperature at the bottom of the tank has reached an approximately constant temperature (76 minutes after the heater was first turned on).

**3.1.1. Stratified Regime ( $B > 0.8$ ).** [10] In the stratified regime [*Davaille*, 1999a, 1999b] (Figures 3a and 3b), the lower layer is hotter than the upper layer and a thermal boundary layer develops at the interface between the two layers. Both layers convect, but remain separated by the density interface. Convection in both layers is characterized by two scales of motion: (i) plumes form at the hot bottom boundary and in the thermal boundary layer associated with the density interface (upper layer); (ii) large-scale circulation in each layer is induced by lateral temperature gradients.

[11] Motions at both scales deform the interface. The large-scale circulation sweeps the dense layer into a broad mound, thereby sustaining lateral temperature gradients. Fluid at the bottom of the lower layer obtains sufficient thermal buoyancy to form rising plumes; these deform the density interface, but cannot penetrate far into the upper layer. Rising plumes are advected laterally along the density interface toward the highest part of the mound, which coincides with the region of upwelling flow in the upper layer. At the same time, plumes originate in the upper layer at the density interface. These plumes are localized directly above the deformations, i.e. the hottest part of the density interface.

[12] When rising plumes detach from the interface they entrain thin tendrils of dense fluid from the lower layer. Simultaneously, large-scale circulation and sinking plumes entrain fluid from the upper layer into the lower layer. Overall, the volume of each layer remains approximately constant throughout this regime. This indicates that the upward and downward fluid flux across the interface is balanced, as we might anticipate for  $\gamma = 1$  on the basis of symmetry arguments.

[13] The thin tendrils of entrained fluid are continuously stretched and thinned by the convective flow, thereby effectively mixing both layers on time scales comparable to or shorter than the time to make a plume. Owing to mixing in both layers,  $B$  decreases

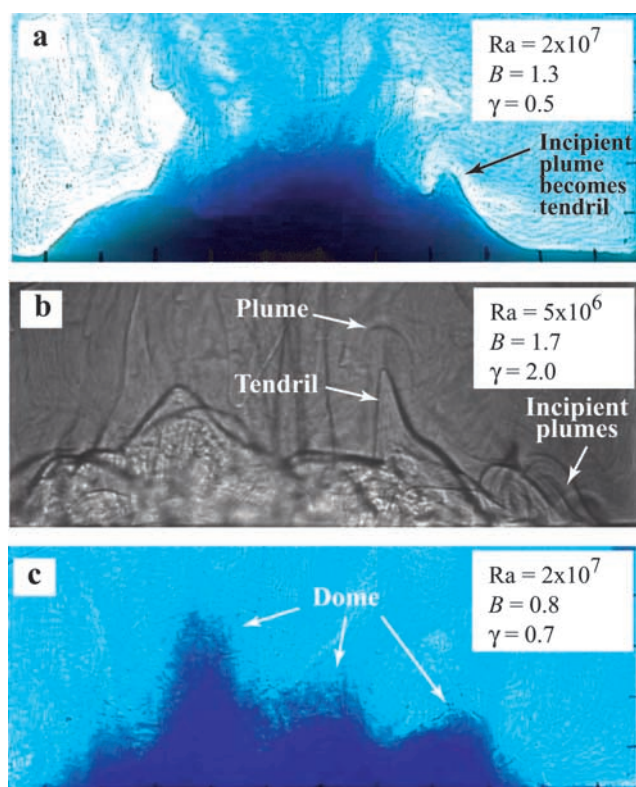


**Figure 3.** Images from a digital video of convection in (a, b) the stratified regime and (c) the doming regime. In (a and c) fluids are corn syrup solutions, in (b) polybutene oils. All fluids are Newtonian.

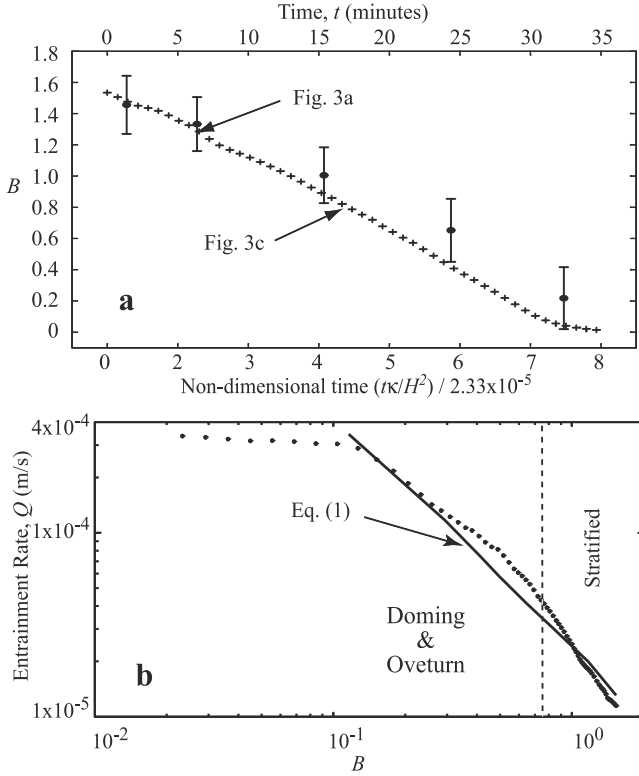


**Figure 4.** Evolution of  $B$  and  $Q$ . (a)  $B$  as a function of time based on temperature (crosses) and luminosity (filled circles) measurements. (b) Volumetric entrainment rate (volume/area per unit time) as a function of  $B$ . The solid line is Equation (1) with  $C = 0.2$  and is calculated using the values of  $B$ ,  $\gamma$ , and  $Ra$  as they evolve during the experiment.

throughout the experiment resulting in a reduced restoring buoyancy force. Consequently, the size of entrained tendrils increases, the amplitude of interface deformations increases, and large-scale flow weakens.

**3.1.2. Doming and Overtun ( $B < 0.8$ ).** [14] When  $B < 0.8$  the density interface becomes highly deformed (Figure 3c) into broad, dome-like structures that penetrate into the upper layer [Davaile, 1999a]. These domes form the “cores” of rising plumes. At the same time, the large-scale circulation that characterizes the stratified regime weakens and eventually ceases as the temperature difference between the two layers,  $\Delta T_i$ , decreases.

[15] When  $B < 0.2$  there is no large-scale circulation. Entrainment proceeds rapidly and is entirely due to plumes, similar to observations by Olson and Kincaid [1991] at small density ratios. Ultimately the lower layer breaks up and overturns rapidly.

### 3.2. Entrainment

[16] We estimate entrainment rates  $Q$  (upward + downward volume flux per unit area across the density interface) by using temperature measurements. Initially  $\Delta T_i$  is at a maximum, but owing mostly to entrainment and mixing it decreases monotonically throughout the experiment (Figure 2). The conductive heat flux across the interface decreases with time and a significant proportion of heat is advected by fluid flow across the interface. A global heat balance for the lower layer, assuming complete mixing, results in  $q \approx Q\Delta T_i c_p \rho + q_c$ , where  $c_p$  is specific heat and  $q_c$  the conductive heat flux across the interface. Initially  $q_c \approx q$  and we assume that  $q_c$  varies linearly with  $\Delta T_i$  until both fluids are completely mixed and  $q_c = \Delta T_i = 0$ . Solving for  $Q$  and time-integrating Equations 7 and 8 of Davaile [1999b] gives  $\Delta\rho$  and hence  $B$  over the duration of the experiment (Figure 4).

[17] Davaile [1999b] showed that it is possible to estimate dye concentration, or equivalently density, based on light absorption measurements. To confirm our estimates of  $B$  based on temperature measurements, we measure the relative luminosity of the two fluids using Photoshop<sup>®</sup>. Initially, when both fluids are unmixed, the difference in luminosity is at a maximum. When both fluids are completely mixed, luminosities for both fluids are identical. Since initial and final density differences are known, density differences can be estimated from luminosity measurements made at different times during the experiment. The two independent estimates of density are consistent (Figure 4a).

[18] Figure 4b shows the volumetric entrainment rate per unit area as a function of  $B$ . Figure 4b also shows the scaling theory presented by Davaile [1999a], which is derived from a balance of buoyancy and viscous forces,

$$Q = C\kappa H^{-1} B^{-2} Ra^{1/3} \frac{1}{1 + \gamma B^{-1}}. \quad (1)$$

$C$  is an experimentally determined constant, with value  $C = 0.2$  for  $B > 0.2$  (Figure 4a). The curve obtained from Equation (1) shown in Figure 4b allows  $\gamma$ ,  $B$  and  $Ra$  to change as they evolve during the course of the experiment. Our value of  $C$  is two orders of magnitude larger than that reported in Davaile [1999a] due to an error made in the presentation of results [Davaile, personal communication]. Furthermore, our entrainment rate  $Q$  differs from Davaile [1999a], where it represents fluid flux from bottom to top layer only.

[19] For  $B < 0.2$  the hot plumes of dense fluid can penetrate fully into the ambient fluid. Now the entrainment rate approaches a constant that is determined by the rate at which hot plumes are formed.

## 4. Implications for the Earth’s Mantle

[20] If the Earth’s lower mantle was initially layered, can the stratification persist for the age of the Earth? Our experiments have a heated, no-slip bottom boundary. Unlike the Earth, they are not heated internally or stirred by subducting plates (rather, we designed our experiments to make the measurement of entrainment rates as straightforward as possible). Entrainment rates scale with convective velocities, which in turn scale as  $Ra$  to a low power ( $< 1$ ). Hence, uncertainty in  $Ra$  or the effects of internal heating should not alter our general conclusions. Assuming that  $\gamma$  is close to unity, it is possible to apply results from our experiments to

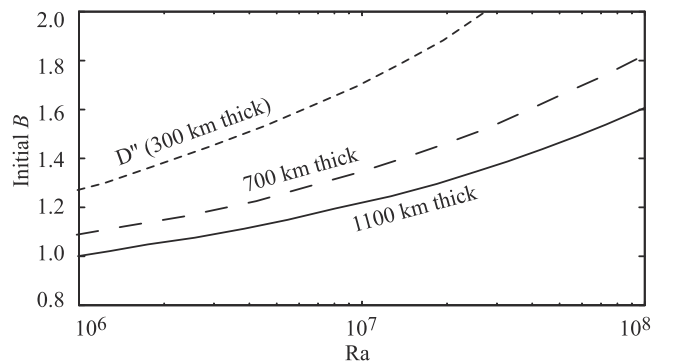


**Figure 5.** Parameters ( $Ra$ , initial  $B$ ) for which a hypothetical dense layer (assumed spherical geometry, constant  $Ra$  and no internal heating) of given initial thickness (1100 km, 700 km, 300 km) will remain in the stratified regime for 4.5 Ga. Curves are based on time integration of the change in density (Equations 7 and 8 of Davaile [1999b], where  $Q$  is based on Equation 1) so that the time dependence of  $Q$ , due to evolving  $B$ , is taken into account.

estimate the temporal evolution of a hypothetical dense lower-mantle layer with given initial  $B$  and initial volume.

[21] Each curve in Figure 5 represents the values of  $Ra$  and initial  $B$  for which a chemically dense lower-mantle layer of given initial thickness is likely to persist in the stratified regime ( $B > 0.8$ ) for the age of the Earth. Similar to previous studies [e.g., Sleep, 1988; Davaille, 1999a] we find that a layer approximately 300 km thick (equivalent to the thickness of  $D''$ ) would, assuming no replenishment, require a relatively large density contrast (approximately 2% or more, assuming  $\Delta T \sim 10^3 K$  and  $\alpha \sim 10^{-5} K^{-1}$ ) to remain in the stratified regime for the age of the Earth for  $Ra > 10^7$ . The longevity of a compositionally distinct layer is therefore critically dependent on the initial density difference and layer thickness.

[22] Figure 5 suggests that for modest initial density differences (<2%) convection can remain stratified for a mid-lower mantle layer. However, the dense layer would be highly deformed and may provide a physical explanation for superswells [Forte and Mitrovica, 2001]. Plumes originating at the thermal boundary layer associated with the density interface are advected laterally along the density interface. We should thus expect plumes to be more frequent in the vicinity of upwelling regions (e.g. superswells).

[23] In summary, if the initial value of  $B$  is greater than about 1, a “stratified” mantle (but with a highly deformed interface) may be able to persist for the age of the Earth [Davaille, 1999a, 1999b; Kellogg et al., 1999]. This is true even in the absence of a large viscosity contrasts.

[24] **Acknowledgments.** Supported by NSF EAR-0124972 and the Miller Institute for Basic Research in Science. We thank D. Stegman, A. Davaille and two reviewers for comments.

## References

- Becker, T. W., J. B. Kellogg, and R. J. O’Connell, Thermal constraints on the survival of primitive blobs in the lower mantle, *Earth Planet. Sci. Lett.*, 171, 351–365, 1999.
- Davaille, A., Simultaneous generation of hotspots and superswells by convection in a heterogeneous planetary mantle, *Nature*, 402, 756–760, 1999a.
- Davaille, A., Two-layer thermal convection in miscible viscous fluids, *J. Fluid Mech.*, 379, 223–253, 1999b.
- Forte, A. M., and J. X. Mitrovica, Deep-mantle high-viscosity flow and thermochemical structure inferred from seismic and geodynamic data, *Nature*, 402, 1881–1884, 2001.
- Grand, S. P., R. D. van der Hilst, and S. Widiyantoro, Global seismic tomography: A snapshot of convection in the Earth, *GSA Today*, 7, 1–7, 1997.
- Hunt, D. L., and L. H. Kellogg, Quantifying mixing and age variations of heterogeneities in models of mantle convection: Role of depth-dependent viscosity, *J. Geophys. Res.*, 106, 6747–6759, 2001.
- Kellogg, L. H., B. H. Hager, and R. D. van der Hilst, Compositional stratification in the deep mantle, *Science*, 410, 1049–1056, 1999.
- Olson, P., and C. Kincaid, Experiments on the interaction of thermal-convection and compositional layering at the base of the mantle, *J. Geophys. Res.*, 96, 4347–4354, 1991.
- Saltzer, R. L., R. D. van derHilst, and H. Karason, Comparing P and S wave heterogeneity in the mantle, *Geophys. Res. Lett.*, 28, 1335–1338, 2001.
- Schubert, G., D. L. Turcotte, and P. Olson, *Mantle Convection in the Earth and Planets*, Cambridge University Press, 2001.
- Sleep, N. H., Gradual entrainment of a chemical layer at the base of the mantle by overlying convection, *Geophys. J.*, 95, 437–447, 1988.
- Tackley, P. J., Three-dimensional simulations of mantle convection with a thermal-chemical boundary layer:  $D''$ , in *The Core-Mantle Boundary Region*, edited by M. Gurnis et al., Geodynamics Series, 28, 231–253, 1998.
- Turcotte, D. L., D. Paul, and W. M. White, Thorium-uranium systematics require layered mantle convection, *J. Geophys. Res.*, 106, 4265–4276, 2001.
- van Keken, P. E., and S. J. Zhong, Mixing in a 3D spherical model of present-day mantle convection, *Earth Planet. Sci. Lett.*, 171, 533–547, 1999.

H. M. Gonnermann, A. M. Jellinek, and M. Manga, Earth and Planetary Science, 307 McCone Hall, Berkeley, CA 94720-4767, USA. (hmg@seismo.berkeley.edu)